New Biotechnology • Volume 29, Number 5 • June 2012

ELSEVIER



# Monitored whole gene *in vitro* evolution of an anti-hRaf-1 affibody molecule towards increased binding affinity

**Sebastian Grimm, Samaneh Salahshour and Per-Åke Nygren**

Division of Molecular Biotechnology, Royal Institute of Technology, SE-106 91 Stockholm, Sweden

**The use of library technologies for the generation of affinity proteins often includes an affinity maturation step, based on the construction of secondary libraries from which second generation variants with improved affinities are selected. Here, we describe for the first time the affinity maturation of affibody molecules based on step-wise *in vitro* molecular evolution, involving cycles of error-prone PCR (epPCR) amplification for the introduction of diversity over the entire 58-residue three-helix bundle structure and ribosome display (RD) for the selection of improved variants. The model affibody molecule for the process was $Z_{RAF322}$, binding with a 1.9 μM equilibrium dissociation constant ($K_D$) to human Raf-1 (hRaf-1), a protein kinase of central importance in the MAPK/ERK proliferation pathway. The molecular evolution process was followed on both gene and protein levels via DNA sequencing and a biosensor-based binding analysis of pools of selected variants. After two cycles of diversification and selection, a significant increase in binding response of selected pools was seen. DNA sequencing showed that a dominant alanine to valine substitution had been effectively enriched, and was found in 83% of all selected clones, either alone or in combination with other enriched substitutions. The evolution procedure resulted in variants showing up to 26-fold increases in affinity to the hRaf-1 target. Noteworthy, for the two variants showing the highest affinities, substitutions were also found in affibody framework positions, corresponding to regions of the protein domain not addressed by traditional affibody molecule affinity maturation strategies. Interestingly, thermal melting point ($T_m$) analyses showed that an increased affinity could be associated with both higher and lower $T_m$ values. All investigated variants showed excellent refolding properties and selective binding to hRaf-1, as analysed using a multiplexed bead-based binding assay, making them potentially valuable affinity reagents for cell biology studies.**

## Introduction

The use of non-immune principles for the generation of novel binding proteins from large libraries has become an important route for development of reagents for diagnostics, biotechnology and therapy [1]. This involves binding proteins of different structural classes, including antibody fragments and so-called scaffold proteins of different sizes and origins [2,3]. Typically, libraries are constructed by combinatorial genetic engineering, followed by selection or screening of binders to a given target under stringent conditions using one of several available protein display technologies [3]. Affinities of selected binders for their targets can differ widely, depending on several parameters including binder class, library size, selection procedures and target characteristics. First generation binders obtained from general and unbiased, that is naïve, libraries are frequently subjected to affinity maturation, involving the construction of secondary and more focused libraries from which variants with improved affinities are selected.

*Corresponding author:* Nygren, P.-Å. (perake@biotech.kth.se)



1871-6784/$ - see front matter  doi:10.1016/j.nbt.2011.10.008

As part of the MAPK/ERK signal cascade, the interaction between Ras GTPases and Raf serine/threonine kinases plays a central role in the control of cell proliferation, survival and growth. Mutations in Ras and Raf proteins may lead to an aberrant signalling and are frequently found in various types of cancer cells [4]. Affinity proteins that selectively block the interaction between Ras and Raf proteins may become valuable tools to further dissect the biology of this important pathway. Earlier work has focused on the development of antibody-derived fragments for blocking the interaction between Ras and Raf and also preventing tumourigenesis in a mouse model [5]. We have recently described the selection of affibody molecules to a fragment of hRaf-1 containing the Ras-binding domain (RBD). A $10^9$-sized naïve affibody library was used, constructed by randomisation of 13 positions located to the molecular surface of the first two helices of the three-helix bundle scaffold. One binder, denoted $Z_{RAF322}$ and used as template molecule in the present study, was shown to bind hRaf-1 with a $K_D$ of 1.9 μM and inhibit the interaction between Ras and Raf *in vitro* [6].

In previous attempts to affinity mature affibody binding proteins, secondary libraries have been constructed where typically a subset of the 13 originally randomised positions have been re-randomised according to different strategies, often based on consensus sequences of first generation clones [7,8]. However, such targeted strategies may miss beneficial substitutions in framework or loop positions that can also be important for an improved affinity or stability.

In the present study, we have taken an untargeted and step-wise approach for the affinity maturation of a first generation hRaf-1 binding affibody molecule. Consecutive cycles of error-prone PCR (epPCR) over the entire affibody gene followed by ribosome display (RD) selection have been employed, for the first time opening up for the identification of affinity promoting mutations also outside the 13 originally randomised positions.

## Materials and methods

### General

Standard PCR products were prepared using Phusion DNA polymerase (Finnzymes) and oligonucleotide primers from Eurofins MWG Operon. DNA modifying enzymes were from New England Biolabs. PCR products were purified using the QIAquick DNA purification kit (Qiagen). Vector DNA was prepared using the QIAprep Spin Miniprep kit (Qiagen) and cleaved vector or vector insert DNA was extracted from agarose gel and recovered using the JETQUICK gel extraction kit (Genomed). DNA sequences of all constructs were verified using an ABI Prism 3700 analyzer (Applied Biosystems).

### DNA sequencing

The composition of libraries obtained after epPCR of the $Z_{RAF322}$ gene were analysed by DNA sequencing on an ABI Prism 3700 analyzer (Applied Biosystems) using specific sequencing primers and BigDye™ terminators (Amersham Biosciences). As template, either purified vector or PCR products obtained from randomly picked *Escherichia coli* RR1ΔM15 colonies were used. Sequences were analysed and aligned using Geneious Pro™ (Biomatters).

### Target protein preparation

hRaf-$1_{5\text{-}143}$ was expressed from pAff8c-ABP-hRaf-$1_{5\text{-}143}$ in *E. coli* Bl21(DE3). 100 ml of TSB medium containing 50 mg/l kanamycin and 5 g/l yeast extract was inoculated with 1 ml of a pre-culture, cells were grown at 37°C to an $OD_{600}$ of 0.5, when expression was induced by addition of β-D-thiogalactoside (IPTG, Apollo Scientific Ltd) to 1 mM. After four hours, cells were harvested and protein was purified on two His SpinTrap columns (GE Healthcare) according to the manufacturer's native IMAC protocol. Eluate buffer was exchanged to HBS-E (5 mM HEPES, 150 mM NaCl, 3.4 mM EDTA pH 7.4) and protein purity was confirmed on a reducing NuPAGE® Novex 4–12% Bis–Tris gel (Invitrogen). 430 μg of ABP-hRaf-$1_{5\text{-}143}$ was biotinylated with a 8-fold molar excess of EZ-link™ Sulfo-NHS-LC-biotin (Thermo Fisher Scientific) in a volume of 1 ml for two hours on ice, excess biotin was removed by dialysis against HBS.

### Preparation of DNA constructs

The expression vector pAff35 was prepared by amplifying the $ABD_{35}$ gene [9] using the primers 35-for (5′-GAACTAATGGCTAGCT-TAGCTGAAGCTAAAGTCTTAGCTAACAGAGAACTCGACAAA-TATG-3′; underlined: *Nhe*I recognition site) and 35-rev (5′-AACTTATTCGGATCCCCCTGGAAGTACAGGTTTTCACCGCTAC-CGCCACCAGGTAATGCAGCTAAAATATGCAATTTAAG-3′; underlined: *Bam*HI recognition site) and inserting it between the *Nhe*I and *Bam*HI sites of pAff8c [10]. To yield the expression vector pAffX, encoding a $His_6$-purification handle and a minimum of additional linker residues to avoid a possible perturbation during circular dichroism analysis, the oligonucleotides Nco-for (5′-CATGGGCAG-CAGCCATCATCATCATCATCACTCG-3′) and Bam-rev (5′-GATCC-GAGTGATGATGATGATGATGGCTGCTGCC-3′) were hybridised and the hybridisation product with protruding bases was directly inserted between the *Nco*I and *Bam*HI sites of pAff10c.

### Library preparation for RD (Fig. 1a–e)

The gene of $Z_{RAF322}$ was amplified from pAY442-$Z_{RAF322}$ using the primers Zep-for2 (5′-AAGATGACGATGATAAAACGTCGACCGTA-GACAACAAATTCAACAAAGAA-3′) and Zep-rev2 (5′-ATTGGCCTT-GATATGAGCTCGAGCTTTTCGGCGCCTGAGCATCATTTAG-3′). The product was purified, quantified and 1 pg served as template in a subsequent, epPCR reaction. The GeneMorph® II Random Mutagenesis Kit (Stratagene) was used according to manufacturer's recommendations in combination with primers Zep-for (5′-AAGATGACGATGATAAAACGTCGAC-3′; underlined: *Sal*I recognition site), Zep-rev (5′-ATTGGCCTTGATATGAGCTC-GAG-3′; underlined: *Sac*I recognition site), 30 amplification cycles and 50°C annealing temperature. 25 ng of resulting epPCR product was inserted between the *Sal*I and *Sac*I recognition sites of 50 ng pRD2-bla-H3 [11]. A small aliquot of the ligation reaction was transformed to *E. coli* to evaluate the mutation spectrum and frequency of the library and 25% were used as template for the preparation of library DNA cassettes for RD selection, using the primers RD-for and RD-rev9, as described previously [11].

### Ribosome display

Library mRNA and ternary affibody–ribosome–mRNA (ARM) complexes were prepared as described previously [11]. ARM complexes were incubated for one hour with 80 nM (cycle 1) or 20 nM (cycle 2) biotinylated ABP-hRaf-$1_{5\text{-}143}$ at 4°C (cycle 1 route I) or ambient room temperature (cycle 1 route II, cycle 2 route I/II) while shaking. The mixture was subsequently added to 0.5 mg NeutrAvidin-coated,

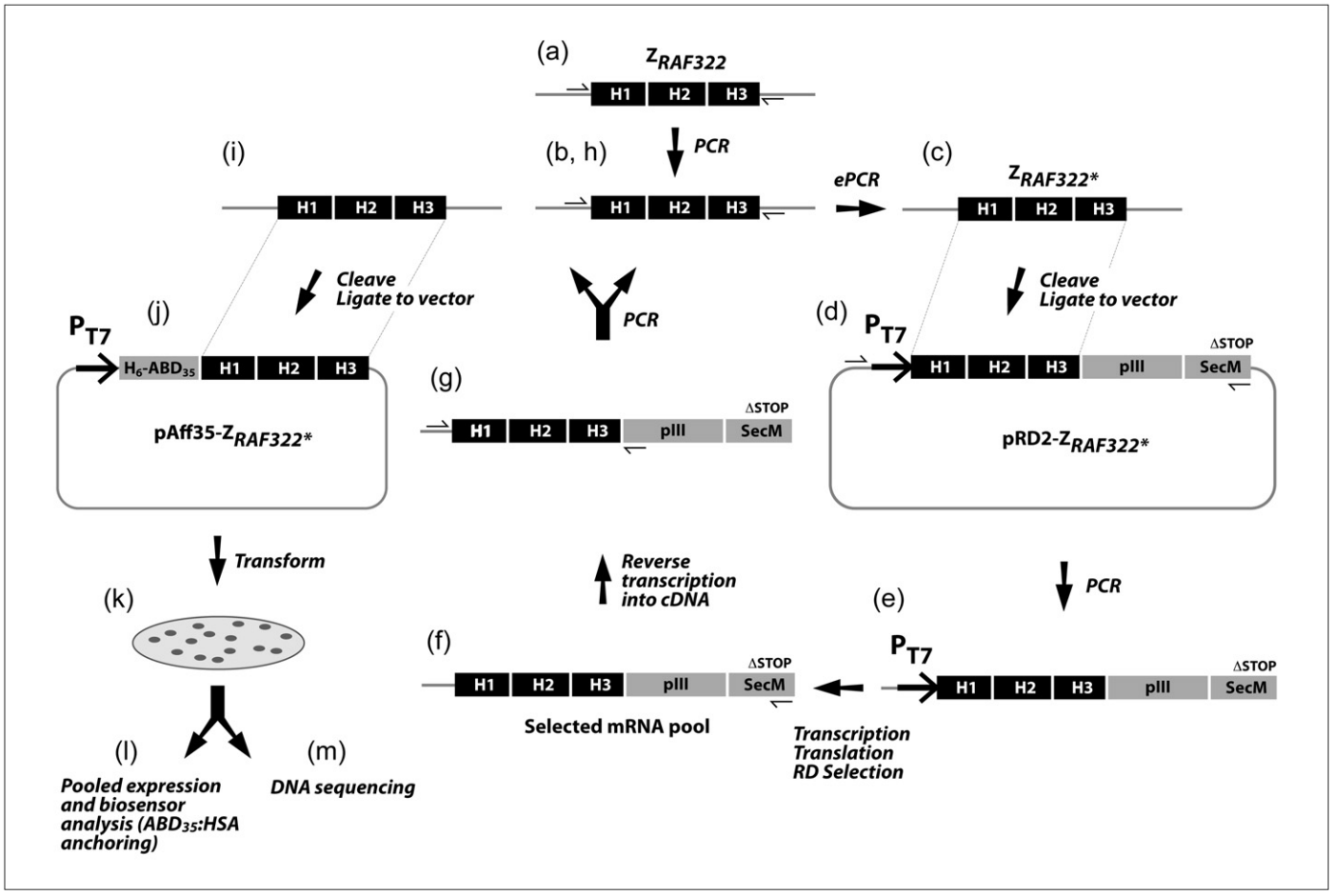


**FIGURE 1**

Schematic overview of the affinity maturation strategy. The gene encoding $Z_{RAF322}$ was amplified from circular DNA template **(a)** to yield linear DNA template **(b)** for a subsequent epPCR reaction **(c)**. The pool of mutated $Z_{RAF322}$-clones ($Z_{RAF322*}$) was inserted in vector pRD2 to introduce promoter ($p_{T7}$) and pIII-SecM spacer protein for RD **(d)**. Gene cassettes devoid of STOP-codon and including promoter, $Z_{RAF322*}$ and spacer were amplified, transcribed and translated *in vitro* for RD selection **(e, f)**. Selected mRNA molecules were reverse transcribed **(g)** and PCR-amplified to obtain template for the subsequent selection cycle **(h)** or for ligation to a hexahistidine-albumin binding domain ($H_6$-$ABD_{35}$) tag in an expression vector **(i, j)**. For pool and clonal analysis, *E. coli* cells were transformed and sequenced **(k, m)** or induced for expression of tagged $Z_{RAF322*}$ and capture of $H_6$-$ABD_{35}$-$Z_{RAF322*}$ on a biosensor for pool phenotypic analysis **(l)**.

blocked Dynabeads® M280 (Invitrogen) and the suspension was incubated for 15 min at 4°C (cycle 1 route I) or room temperature (cycle 1 route II, cycle 2 route I/II) while shaking. Beads were washed 6 times as described previously [11]. During the last wash, beads were incubated in WBT for 6 min (cycle 1) or one hour (cycle 2), before discarding the supernatant. The mRNA was eluted, recovered and reverse transcribed. To generate DNA template for another round of epPCR and RD selection, 25% of the reverse transcription product was PCR-amplified using the primers Zep-for, Zep-ref and 35 amplification cycles (Fig. 1g,h).

### *Vector and cell lysate preparation for genotypic and phenotypic selection analyses*

For analyses of the selection outputs (Fig. 1i–m), 25% of the reverse transcript was amplified using the primers Zsub-for6 (5′-AAGATGACGATGATAAAACGGATCCCGTAGAC-3′; underlined: *Bam*HI recognition site) and Zsub-rev4 (5′-ATTGGCCTTGATATAAGCTTTAGCTTTTCG-3′; underlined: *Hin*dIII recognition site) and inserted between the *Bam*HI and *Hin*dIII sites of pAff35 to obtain pAff35-$Z_{RAF322*}$, where * stands for different variants. The ligation reaction was purified on a QIAquick DNA purification column (Qiagen) and transformed to *E. coli* RR1ΔM15 cells to obtain single colonies for sequencing of individual clones. For the phenotypic pool analysis, 25 μl of electrocompetent *E. coli* Bl21(DE3) cells were transformed with an aliquot of the purified ligation reaction in a 0.1 cm cuvette, using a Bio-Rad MicroPulser (Bio-Rad) and a voltage of 2.4 kV for 1.1 ms. Transformed cells were immediately mixed with SOC recovery medium and incubated for one hour at 37°C while shaking. 10 ml of TSB medium containing 50 mg/l kanamycin was inoculated with the transformants and grown over night at 37°C. Proteins were produced in 100 ml culture volume as described for ABP-hRaf-$1_{5\text{-}143}$. Cell pellets were suspended in 5 ml HBS buffer and disrupted by sonication. The cell debris was sedimented (29,000 × *g*, 4°C, 30 min) and the supernatant filtered (0.45 μm) and stored at −20°C.

### *Protein production, purification and biotinylation*

For the analysis of individual $Z_{RAF322}$ variants, pAff35-$Z_{RAF322*}$ was prepared and cleaved using *Hin*dIII and *Bam*HI. The affibody molecule-encoding fragments were inserted between the *Bam*HI

and *Hin*dIII sites of pAffX and pAffX-$Z_{RAF322*}$ was prepared and transformed to *E. coli* Rosetta (DE3) cells. Proteins were produced in 150 ml medium as described in the previous sections, with the following modification: after induction of protein expression, cells were grown at 25°C over night. $Z_{RAF322}$ variants were purified using denaturing IMAC affinity chromatography, as described previously [11]. Purified proteins were re-folded by dialysis against 1 M urea in PBS, followed by dialysis against PBS, only. Protein purity was confirmed on a reducing Mini-PROTEAN TGX Any kD® gel (Bio-Rad) according to the suppliers instructions. For bead-based binding selectivity analyses, 0.5 mg of each $Z_{RAF322}$ variant was biotinylated using a 2-fold molar excess of EZ-link™ Sulfo-NHS-LC-biotin in a volume of 0.5 ml for two hours on ice, and excess biotin was removed by dialysis against PBS. A majority of the molecules was found to contain one or two biotin groups, as determined by mass spectrometry.

### *Biosensor analyses*

All biosensor binding analyses were performed on a BIAcore 2000 or 3000 instrument (GE Healthcare) at 25°C in HBS-ET (HBS-E containing 0.005% Tween 20) running and sample buffer at a flowrate of 20 μl/min unless stated otherwise. 10 μl of 10 mM glycine–HCl pH 2 was used for surface re-generation, followed by 10 min stabilisation time before subsequent measurement cycles. For phenotypic pool analyses from cell lysates, 9000 RU human serum albumin (HSA) were immobilised on a CM5 sensorchip surface (GE Healthcare). 100 μl of 1:10 dilutions of $ABD_{35}$-affibody molecule containing cell lysates was flowed over the HSA surface and allowed to dissociate for 3 min, until 50 μl of a 200 nM analyte GST-hRaf-1 RBD (Millipore) sample was flowed over the same surface for detection of binding to the captured affibody variants. For data analysis, blank surface-referenced traces were normalised to an arbitrary 1000 RU before antigen injection, and further referenced by subtraction of traces obtained from cell lysate injections followed by HBS-ET instead of analyte injections. For the binding analysis of individual, selected affibody clones, 2950 RU of ABP-hRaf-$1_{5\text{-}143}$ were immobilised on another CM5 sensorchip. For single-concentration binding analyses, 100 μl of 1 μM affibody variants were flowed over the surface. For kinetic measurements, 160 μl of concentration series ranging from 8 μM to 15.6 nM was injected at 40 μl/min in duplicate, respectively, and samples were allowed to dissociate for 4 min. To correct for systematic deviations and bulk buffer effects, both reference blank surface signal and a trace obtained from a buffer sample were subtracted [12]. For the calculation of kinetic rate constants and $K_D$, traces were fitted using a 1:1 Langmuir binding model (BIAevaluation 3.2 software (GE Healthcare)).

### *CD measurements*

CD spectra and melting curves of selected affibody molecules and $Z_{WT}$ reference were collected on a Jasco 810 spectropolarimeter (Jasco) at a protein concentration of 62 μM in 200 μl PBS pH 7.4. Firstly, a spectrum ranging from 250 to 195 nm was recorded at 25°C. Secondly, the circular dichroism at a fixed wavelength of 221 nm was recorded while gradually increasing the temperature from 20°C to 90°C. Thirdly and after the sample had equilibrated to 25°C, a second spectrum ranging from 250 to 195 nm was collected. The obtained melting curves were normalised and the melting temperatures $T_m$ were obtained from midpoints of the transitions.

## Results

A study was performed to investigate molecular evolution principles, that is consecutive cycles of undirected genetic diversification followed by phenotypic selection, for the affinity maturation of $Z_{RAF322}$, a previously described affibody molecule with a $K_D$ of approximately 1.9 μM for the RBD of human Raf-1 (hRaf-1). A combination of epPCR and RD selection was applied. The affinity maturation process was monitored by an analysis of the target binding of representative molecule pools on a surface plasmon resonance (SPR) biosensor. The procedure is illustrated in Fig. 1.

### *Affibody library preparation and selection*

Initially, diversity was introduced within the entire three-helix bundle domain structure of $Z_{RAF322}$, using an error-prone, thermostable DNA polymerase (Fig. 1b,c). This is in contrast to previously described strategies for affibody affinity maturation, focusing a re-diversification to a subset of the 13 originally randomised amino acid positions. The amount of template DNA and PCR cycle numbers had been titrated to yield on average 1–2 amino acid substitutions per gene fragment, a desired mutagenesis level for this study (data not shown).

For the phenotypic selection of $Z_{RAF322}$ mutants with improved binding properties, the library was subjected to RD selection towards a recombinant fragment of hRaf-1 that contains the RBD fused to an albumin binding protein (ABP-hRaf-$1_{5\text{-}143}$). The selection stringency was increased in consecutive cycles by decreasing the antigen concentration and increasing the washing time. Two parallel selection routes were investigated that differed in the temperature used during biopanning: a standard 4°C, previously described to be necessary to maintain the integrity of fragile ternary complexes, as opposed to ambient room temperature. We reasoned that the latter condition was feasible given the high stability reported for ternary complexes formed by translation of polypeptides encompassing ARM-complex stabilising and *E. coli* secretion monitoring protein (SecM)-derived C-terminal elements [13].

### *Binding analyses of selected affibody pools*

To allow for monitoring of the binding properties of selected pools, affibody molecules were fused to $ABD_{35}$, an engineered 5 kDa serum albumin binding domain showing sub-picomolar affinity to HSA [9]. Pools of affibody fusion proteins were injected over immobilised HSA on a biosensor surface. The strong interaction between $ABD_{35}$-affibody fusions and HSA resulted in a stable capture of the pools of selected affibody variants. The equilibrium binding response obtained after injection of an hRaf-1 RBD glutathione S-transferase fusion (GST-hRaf-1 RBD) to the captured pools provided a relative measure for the pool binding properties (Fig. 2a). A comparison to the response obtained for a cell lysate containing the original $Z_{RAF322}$ clone fused to $ABD_{35}$ showed that the first round of mutagenesis and selection had not led to any significant improvement of the target binding ability, regardless of the temperature used during biopanning (Fig. 2b,d). In the analysis of the pools from the second selection cycle, however, approximately twofold higher binding responses to the hRaf-1

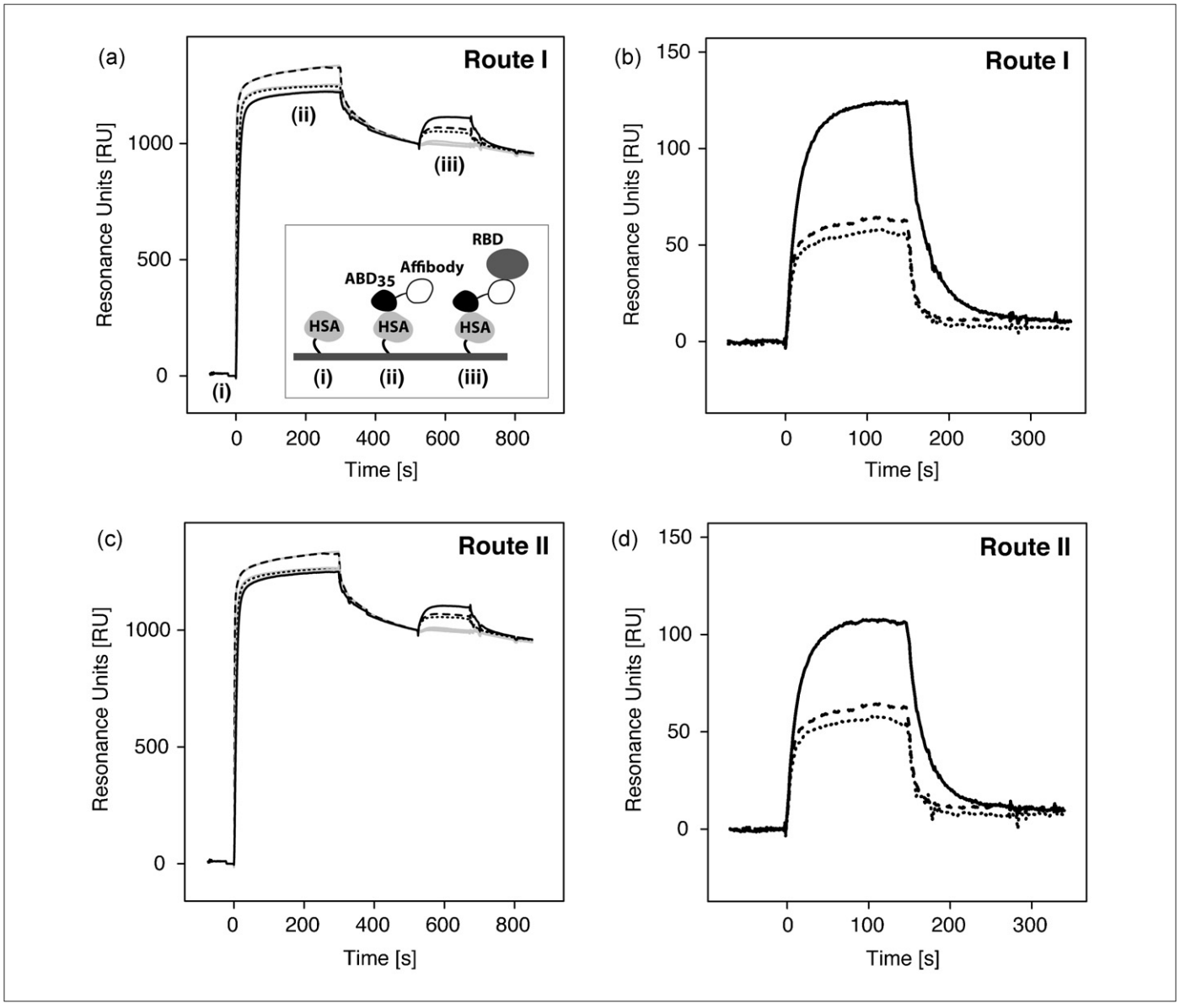


**FIGURE 2**

Biosensor-based pool analysis of relative target affinity during selection process. *E. coli* cell lysates containing pools of mutated $ABD_{35}$-$Z_{RAF322}$ clones obtained after selection cycle 1 (black dotted traces) or selection cycle 2 (black solid traces) from either route I **(a, b)** or route II **(c, d)** were injected over an HSA-surface (ii), respectively, followed by injection of the antigen GST-hRaf-1 RBD (iii). *E. coli* cell lysate containing $ABD_{35}$-$Z_{RAF322}$ only (same black dashed trace for routes I and II) was included as comparison. For reference subtraction, a duplicate of each cell lysate sample was flowed over the HSA surface, followed by injection of a buffer sample (grey solid traces). All traces were normalised to 1000 RU at the point of antigen injection. Traces before reference subtraction are shown in (a) and (c). Corresponding traces obtained from antigen injections after reference subtraction are shown in (b) and (d).

RBD analyte were observed when compared to the paternal $Z_{RAF322}$ clone. This significant difference indicated that both cycle two pools contained sufficiently large fractions of $Z_{RAF322}$ variants with increased affinities to hRaf-1. To analyse selected pools from cycle 1 and 2 further, the affibody molecule encoding gene inserts of 96 clones from each pool were subjected to DNA sequencing.

### *Sequence analyses of selected affibody variants*

After cycle 1, 40–50% of the clones from both routes still corresponded to the original $Z_{RAF322}$ sequence. For the rest of the clones, typically 1–3 mutations per clone were relatively evenly spread over the entire affibody molecule. A specific mutation (A27V) was seen in 11% of selected clones from both routes, indicating an involvement in the selection process. Strikingly, after a second selection cycle the A27V substitution was seen in 83% of the clones, accompanied by other relatively abundant substitutions such as F5Y (4%), N10Y (10%), A12V (7%) and I31V (4%) (Supplementary figure S1). Notably, positions 12 and 31 do not belong to the group of 13 originally randomised affibody library positions [6]. Four variants, denoted $Z_{RAF322:01}$ to $Z_{RAF322:04}$ and representing different combinations of the most frequently observed substitutions, were chosen for further analyses as single clones (Fig. 3b). All four variants were confirmed to be monomeric in solution (Supplementary figure S2) and showed higher binding response

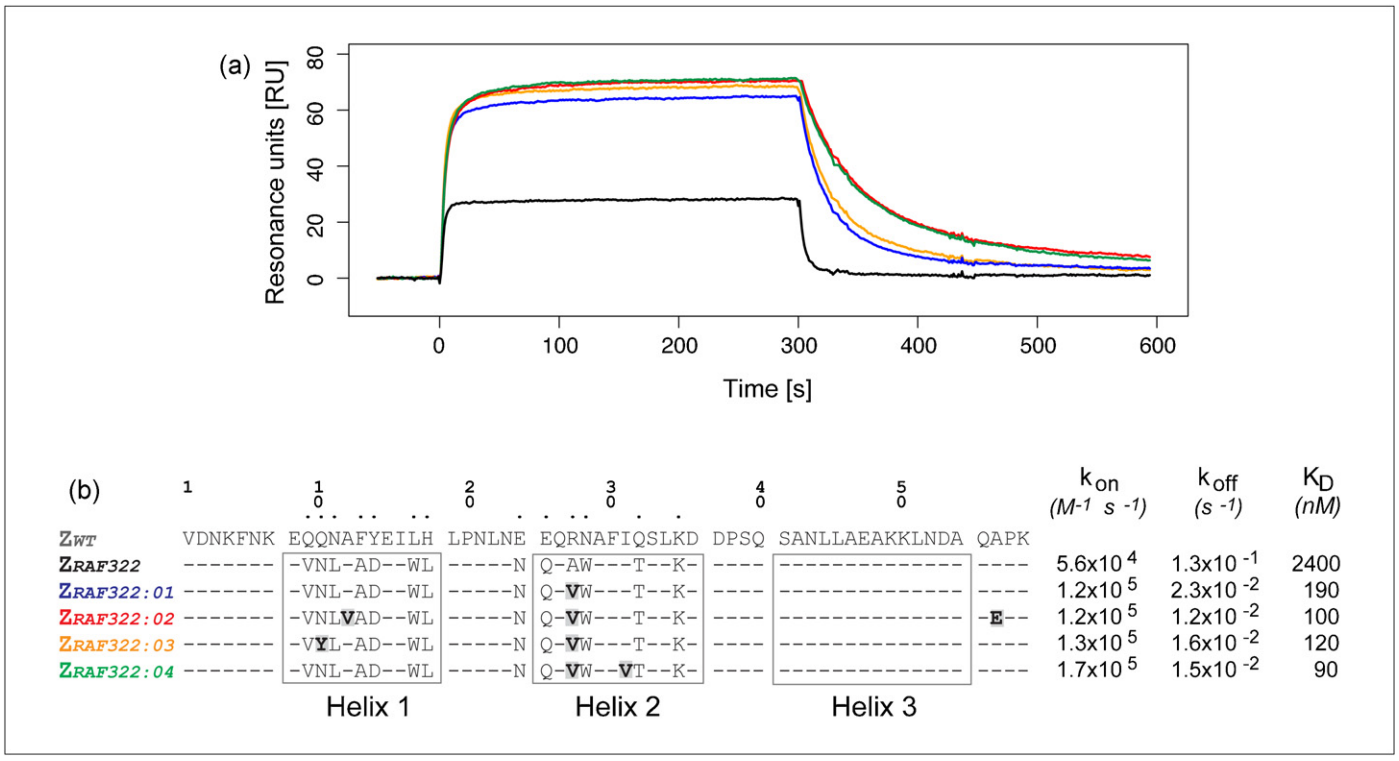


(b)

| | 1 | 10 | 20 | 30 | 40 | 50 | $k_{on}$ ($M^{-1}$ $s^{-1}$) | $k_{off}$ ($s^{-1}$) | $K_D$ (nM) |
|---|---|---|---|---|---|---|---|---|---|
| $Z_{WT}$ | VDNKFNK | EQQNAFYEILH | LPNLNE | EQRNAFIQSLKD | DPSQ | SANLLAEAKKLNDA | QAPK | | | |
| $Z_{RAF322}$ | ------- | -VNL-AD--WL | -----N | Q-AW---T--K- | ---- | -------------- | ---- | $5.6x10^4$ | $1.3x10^{-1}$ | 2400 |
| $Z_{RAF322:01}$ | ------- | -VNL-AD--WL | -----N | Q-**V**W---T--K- | ---- | -------------- | ---- | $1.2x10^5$ | $2.3x10^{-2}$ | 190 |
| $Z_{RAF322:02}$ | ------- | -VNL**V**AD--WL | -----N | Q-**V**W---T--K- | ---- | -------------- | -**E**-- | $1.2x10^5$ | $1.2x10^{-2}$ | 100 |
| $Z_{RAF322:03}$ | ------- | -V**Y**L-AD--WL | -----N | Q-**V**W---T--K- | ---- | -------------- | ---- | $1.3x10^5$ | $1.6x10^{-2}$ | 120 |
| $Z_{RAF322:04}$ | ------- | -VNL-AD--WL | -----N | Q-**V**W--**V**T--K- | ---- | -------------- | ---- | $1.7x10^5$ | $1.5x10^{-2}$ | 90 |

Helix 1 Helix 2 Helix 3

**FIGURE 3**

Characterisation of affinity matured affibody variants. **(a)** Overlay plot of biosensor response traces for the parental $Z_{RAF322}$ (black), $Z_{RAF322:01}$ (blue), $Z_{RAF322:02}$ (red), $Z_{RAF322:03}$ (orange) and $Z_{RAF322:04}$ (green) obtained after injection of 1 $\mu$M solutions of the respective variants over a 2950 RU ABP-hRaf-$1_{5-143}$-containing biosensor surface. **(b)** Sequences and binding parameters of selected $Z_{RAF322}$ variants. The wild type Z domain sequence ($Z_{WT}$) is shown as reference. Dots indicate positions randomised in the library for selection of $Z_{RAF322}$. Boxes indicate positions corresponding to the three $\alpha$-helices of the wild type Z domain. Mutated amino acid positions in $Z_{RAF322}$ variants are written in bold. Kinetic rate constants ($k_{on}$, $k_{off}$) and $K_D$ values are given to the right.

values and slower dissociation rates from ABP-hRaf-$1_{5-143}$ than the parental $Z_{RAF322}$ clone (Fig. 3a). Affinity determinations confirmed that all variants bound with 13–27-fold increased affinities to ABP-hRaf-$1_{5-143}$, corresponding to $K_D$ values in the range 190–90 nM. It could be concluded that the major improvement was seen in the off-rate kinetics values (Fig. 3a,b). The dominant A27V substitution alone accounted for a 13-fold increase in affinity, which in combination with one additional substitution in either position 12 (A12V) or 31 (I31V) resulted in a further approximately twofold affinity increase.

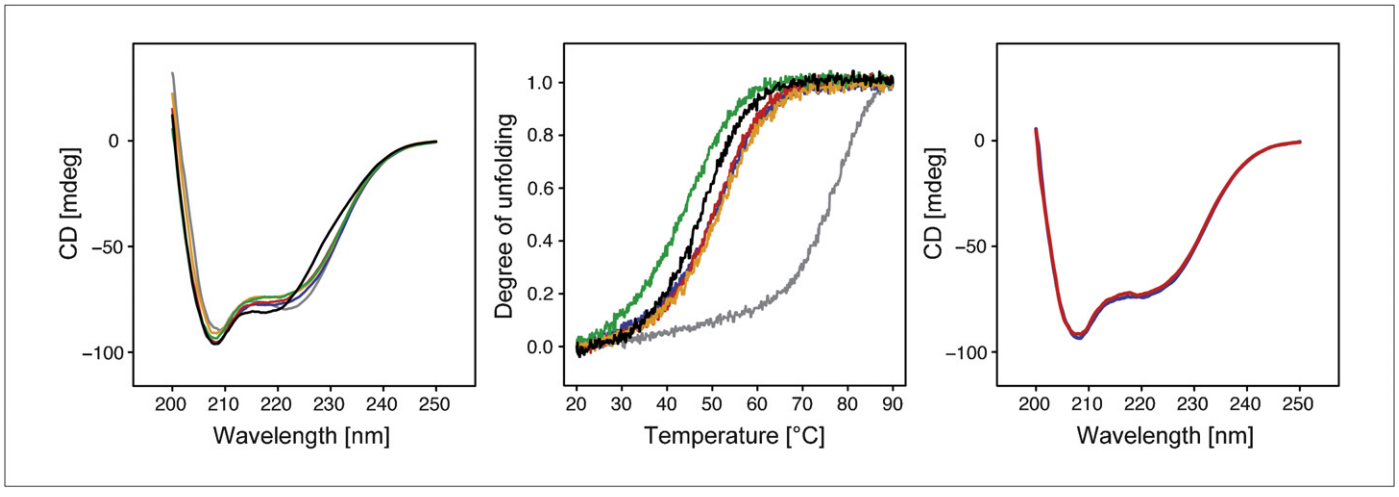


**FIGURE 4**

Secondary structure content, thermal melting point and refolding analyses. Circular dichroism (CD) data were recorded in PBS at pH 7.4 and a protein concentration of 62 $\mu$M. **(a)** Overlay of CD spectra recorded at a constant temperature of 25°C for $Z_{RAF322}$ (black), $Z_{RAF322:01}$ (blue), $Z_{RAF322:02}$ (red), $Z_{RAF322:03}$ (orange), $Z_{RAF322:04}$ (green), and $Z_{WT}$ (grey) samples before thermal melting. **(b)** Normalised thermal melting curves recorded at 221 nm. **(c)** CD spectra of $Z_{RAF322:04}$, either before (blue) or after (red) thermal melting.

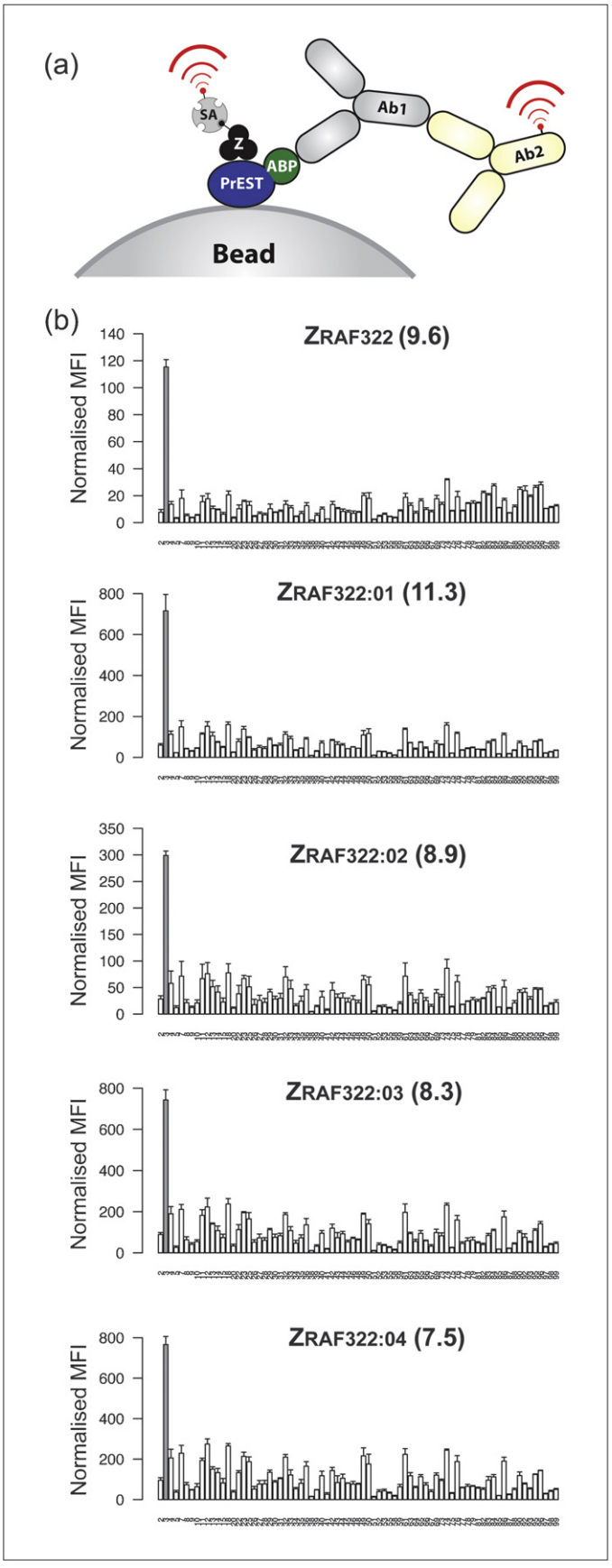


**FIGURE 5**

Analysis of affibody binding selectivity using a collection of 77 recombinant human protein fragment controls (PrESTs). **(a)** PrESTs fused to an albumin binding ABP-tag were coupled to colour-coded beads. For each bead ID, median fluorescence intensities (MFI) obtained from an anti-ABP (Ab1) and labelled secondary (Ab2) antibody served as an estimate for coupled protein levels (data not shown). MFI obtained from biotinylated affibody variants (Z) and labelled streptavidin (SA) were normalised with respect to the corresponding ABP-signals. **(b)** Normalised MFI signals obtained from affibody variants binding to the different PrESTs are plotted against bead IDs. The grey bar of bead ID3 indicates the normalised MFI signal obtained from antigen ABP-hRaf-$1_{5\text{-}143}$-coated beads, respectively. The corresponding mean signal/background ratios are denoted in brackets and standard deviations obtained from triplicate measurements are indicated as error bars.

### *CD measurements and binding selectivity analyses of single affibody variants*

The contents of α-helical secondary structure elements of the affinity matured variants were tested using circular dichroism analysis, and compared to both the wild type Z domain and the parental $Z_{RAF322}$ variant (Fig. 4a). The results suggested that neither the earlier introduced substitutions to generate $Z_{RAF322}$, nor the affinity maturation procedure had significantly affected the folding of any of the helical elements because all variants had very similar overall contents of α-helical secondary structure. The structural stabilities were investigated by thermal melting point analyses (Fig. 4b). $Z_{RAF322:01}$, $Z_{RAF322:02}$ and $Z_{RAF322:03}$ all showed slightly increased thermal stabilities, with $T_m$ values in the range of 50.3–51.4°C which corresponded to a stabilisation of 3–4 degrees compared to $Z_{RAF322}$ showing a $T_m$ of 47.5°C. Interestingly, the variant showing the highest binding affinity, $Z_{RAF322:04}$, showed a $T_m$ value of 43.3°C, approximately four degrees lower than that of $Z_{RAF322}$, indicating that the I31V substitution had a negative effect on the structural stability, yet being associated with a higher target binding affinity. All tested variants produced fully overlapping CD spectra before and after thermal unfolding and cooling, indicating that no aggregation occurred during refolding and that all molecules adapted their initial secondary structure content (Fig. 4c).

Because the observed mutations almost exclusively resulted in substitutions to aliphatic and hydrophobic valine residues, which could lead to an increased unselective binding, the degree of selectivity in the binding to hRaf-1 was investigated. To this end, a panel of 77 different human protein fragments (ABP-hRaf-$1_{5\text{-}143}$ and 76 controls) was utilised as test set as individually coupled to differently colour-coded microbeads (for experimental details, see supplementary section S3). The results show that the parental anti-hRaf-1 $Z_{RAF322}$ clone as well as the investigated affinity matured affibody variants all bound to the ABP-hRaf-$1_{5\text{-}143}$ beads in a selective manner, with high signal to background ratios (Fig. 5).

## Discussion

The present study is the first example for affinity maturation of an affibody molecule involving a non-directed diversification of the entire molecule. Earlier studies have instead involved a reintroduction of variation in a subset of the 13 positions that were originally randomised to construct the naïve library. Even if absolute affinity values obtained in previous affibody affinity maturation studies differ markedly, the up to 26-fold increase in affinity observed here is well in parity with most of the affinity improvements reported, such as 30-fold to HER1 [8], 2200-fold to

HER2 [7], 15-fold to HER3 [14], 8-fold to TNF-α [15] and 10-fold to PDGFR-β [16].

Our primary motivation was to investigate where affinity enhancing substitutions would appear, and what these would be, if the entire sequence was subjected to a 'free', step-wise *in vitro* evolution procedure. Interestingly, substitutions leading to increased affinity were observed both in previously randomised positions, as well as in framework positions. The dominant A27V substitution alone, observed in an originally randomised position, led to a slightly more stable protein and improved the affinity 13-fold. The affinity could further be improved twofold by an isoleucine to valine substitution at framework position 31. Although centrally positioned in the binding face, this residue was not randomised for the construction of the parental affibody library. From analyses of available structures of complexes involving affibody molecules or protein A domains, the I31 position has been speculated to be a 'hot-spot' residue of intrinsic importance for intermolecular interactions [17,18]. However, the I31V substitution observed here suggests that this position may be substituted without negatively affecting but instead improving an interaction, even considering that the binding epitope was originally found by a library member with an isoleucine present at position 31.

Somewhat surprisingly, the increase in affinity seen from the addition of the I31V substitution to the A27V variant was also accompanied by a somewhat decreased structural stability of the protein, even lower than the stability observed for the parental $Z_{RAF322}$ clone. However, it has earlier been shown that affinity maturation of affibody molecules may not result in the most stable variants. The potentially negative effects of a decreased structural stability may in fact be compensated by a thereto linked improved target structure complementarity as shown for Her2-binding affibody molecules [18]. DARPins and anticalins represent two other protein classes based on non-immunoglobulin frameworks that have been subjected to combinatorial protein engineering to construct libraries from which binders to desired target molecules can be selected. Also here, affinity maturation strategies based on whole gene epPCR followed by stringent selection have resulted in the observation of substitutions in framework regions that via different conformational effects of the protein have contributed to an increased affinity [19,20]. The freedom to accept substitutions at certain positions in any class of binding protein may, however, be restricted, as single amino acid changes may affect also other properties inked to its applicability [21,22].

A bias for substitution into valine at positions 12, 27 and 31 was observed. However, for an alanine codon, as in positions 12 and 27 of the parental $Z_{RAF322}$ variant, single epPCR induced mutations in either the first, second or third base of the codon can only result in seven alternative amino acids (V, T, P, S, D, E and G) of which only valine is considered apolar and non-helix-breaking. Therefore, one explanation for the observed valine bias could be a positive effect on affinity from an aliphatic amino acid at interaction surface, here mediated by the only genetic alternative under the conditions used.

It should be noted that the assay is dependent on the ligation efficiency of affibody gene fragments into the expression vector and a high proteolytic stability of protein fusions when expressed in *E. coli*. Otherwise, there is a risk that a fraction of the recombinant proteins of the pool captured via the strong $ABD_{35}$:HSA interaction will be devoid of affibody protein moieties. A further vector development could be to place $ABD_{35}$ C-terminally, preceded by in-frame stop codons that are removed during library gene fragment insertions. Thereby, any religated vectors arising from an earlier incomplete vector digestion would be prematurely truncated and not produce any $ABD_{35}$ tag-only proteins.

In conclusion, the fact that affinity improving substitutions were seen in both framework and previously randomised positions suggests that it may be worthwhile to consider the introduction of a certain degree of variegation outside the traditional set of 13 positions in future affibody molecule maturation projects. The 26-fold affinity increase reported here is well in parity with most previous achievements and the reported affibody variants may become valuable tools for studying the MAPK/ERK signal cascade.

## Acknowledgements

We acknowledge the Swedish Research Council for financial support (Grant No. 621-2009-5755) and Ulrika Qundos, Jochen Schwenk and Per Jonasson for technical assistance.

## Appendix A. Supplementary data

Supplementary data associated with this article can be found, in the online version, at doi:10.1016/j.nbt.2011.10.008.

## References

1 Smothers, J.F. *et al.* (2002) Tech.Sight. Phage display. Affinity selection from biological libraries. *Science* 298, 621–622
2 Holliger, P. and Hudson, P.J. (2005) Engineered antibody fragments and the rise of single domains. *Nat. Biotechnol.* 23, 1126–1136
3 Nygren, P.A. and Skerra, A. (2004) Binding proteins from alternative scaffolds. *J. Immunol. Methods* 290, 3–28
4 Sridhar, S.S. *et al.* (2005) Raf kinase as a target for anticancer therapeutics. *Mol. Cancer Ther.* 4, 677–685
5 Tanaka, T. *et al.* (2007) Tumour prevention by a single antibody domain targeting the interaction of signal transduction proteins with RAS. *EMBO J.* 26, 3250–3259
6 Grimm, S. *et al.* (2010) Selection and characterisation of affibody molecules inhibiting the interaction between Ras and Raf in vitro. *Nat. Biotechnol.* 27, 766–773
7 Orlova, A. *et al.* (2006) Tumor imaging using a picomolar affinity HER2 binding affibody molecule. *Cancer Res.* 66, 4339–4348
8 Friedman, M. *et al.* (2008) Directed evolution to low nanomolar affinity of a tumor-targeting epidermal growth factor receptor-binding affibody molecule. *J. Mol. Biol.* 376, 1388–1402
9 Jonsson, A. *et al.* (2008) Engineering of a femtomolar affinity binding protein to human serum albumin. *Protein Eng. Des. Sel.* 21, 515–527
10 Larsson, M. *et al.* (2000) High-throughput protein expression of cDNA products as a tool in functional genomics. *J. Biotechnol.* 80, 143–157
11 Grimm, S. *et al.* (2011) Ribosome display selection of a murine IgG(1) Fab binding affibody molecule allowing species selective recovery of monoclonal antibodies. *Mol. Biotechnol.* 48, 263–276
12 Myszka, D.G. (1999) Improving biosensor analysis. *J. Mol. Recognit.* 12, 279–284
13 Schaffitzel, C. and Ban, N. (2007) Generation of ribosome nascent chain complexes for structural and functional studies. *J. Struct. Biol.* 158, 463–471
14 Kronqvist, N. *et al.* (2011) Combining phage and staphylococcal surface display for generation of ErbB3-specific Affibody molecules. *Protein Eng. Des. Sel.* 24, 385–396

15 Lofdahl, P.A. and Nygren, P.A. (2010) Affinity maturation of a TNFalpha-binding affibody molecule by Darwinian survival selection. *Biotechnol. Appl. Biochem.* 55, 111–120
16 Lindborg, M. *et al.* (2011) Engineered high-affinity affibody molecules targeting platelet-derived growth factor receptor beta in vivo. *J. Mol. Biol.* 407, 298–315
17 Lendel, C. *et al.* (2006) Structural basis for molecular recognition in an affibody:affibody complex. *J. Mol. Biol.* 359, 1293–1304
18 Eigenbrot, C. *et al.* (2010) Structural basis for high-affinity HER2 receptor binding by an engineered protein. *Proc. Natl. Acad. Sci. U.S.A.* 107, 15039–15044
19 Zahnd, C. *et al.* (2007) A designed ankyrin repeat protein evolved to picomolar affinity to Her2. *J. Mol. Biol.* 369, 1015–1028
20 Binder, U. *et al.* (2010) High-throughput sorting of an Anticalin library via EspP-mediated functional display on the *Escherichia coli* cell surface. *J. Mol. Biol.* 400, 783–802
21 Feldwisch, J. *et al.* (2010) Design of an optimized scaffold for affibody molecules. *J. Mol. Biol.* 398, 232–247
22 Binz, H.K. *et al.* (2003) Designing repeat proteins: well-expressed, soluble and stable proteins from combinatorial libraries of consensus ankyrin repeat proteins. *J. Mol. Biol.* 332, 489–503